INTERNATIONAL JOURNAL OF Experimental Pathology

Int. J. Exp. Path. (2015), 96, 140–150

ORIGINAL ARTICLE

Oxidative and proteolysis-related parameters of skeletal muscle from hamsters with experimental pulmonary emphysema: a comparison between papain and elastase induction

Cláudia R. Brunnquell*, Nichelle A. Vieira†, Laís R. Sábio†, Felipe Sczepanski‡, Alessandra L. Cecchini§, Rubens Cecchini* and Flávia A. Guarnier†

*Laboratory of Pathophysiology and Free Radicals, Department of General Pathology, Universidade Estadual de Londrina, Londrina, Brazil, †Laboratory of Pathophysiology of Muscle Adaptations, Department of General Pathology, Universidade Estadual de Londrina, Londrina, Brazil, ‡Intermunicipal Health Consortium of Pioneer North, Jacarezinho, Brazil and §Laboratory of Molecular Pathology, Department of General Pathology, Universidade Estadual de Londrina, Londrina, Brazil

INTERNATIONAL JOURNAL OF EXPERIMENTAL PATHOLOGY

doi: 10.1111/iep.12121

Received for publication: 27 June 2014
Accepted for publication: 22 January 2015

Correspondence:
Flávia A. Guarnier
Laboratory of Pathophysiology of Muscle Adaptations
Department of General Pathology
Universidade Estadual de Londrina,
Rodovia Celso Garcia Cid, PR 445,
km 380, Campus Universitário
86051-990 Londrina, Brazil
Tel/Fax.: +55-43-33714267
E-mail: faguarnier@uel.br

SUMMARY

The objective of this study was to investigate whether emphysema induced by elastase or papain triggers the same effects on skeletal muscle, related to oxidative stress and proteolysis, in hamsters. For this purpose, we evaluated pulmonary lesions, body weight, muscle loss, oxidative stress (thiobarbituric acid-reactive substances, total and oxidized glutathiones, chemiluminescence stimulated by tert-butyl hydroperoxide and carbonyl proteins), chymotrypsin-like and calpain-like proteolytic activities and muscle fibre cross-sectional area in the gastrocnemius muscles of emphysemic hamsters. Two groups of animals received different intratracheal inductions of experimental emphysema: by 40 mg/ml papain (EP) or 5.2 IU/100 g animal (EE) elastase (n = 10 animals/group). The control group received intratracheal instillation of 300 μl sterile NaCl 0.9%. Compared with the control group, the EP group had reduced muscle weight (18.34%) and the EE group had increased muscle weight (8.37%). Additionally, tert-butyl hydroperoxide-initiated chemiluminescence, carbonylated proteins and chymotrypsin-like proteolytic activity were all elevated in the EP group compared to the CS group, while total glutathione was decreased compared to the EE group. The EE group showed more fibres with increased cross-sectional areas and increased calpain-like activity. Together, these data show that elastase and papain, when used to induce experimental models of emphysema, lead to different speeds and types of adaptation. These findings provide more information on choosing a suitable experimental model for studying skeletal muscle adaptations in emphysema.

Keywords
elastase, emphysema, oxidative stress, papain, proteolysis, skeletal muscle

Chronic obstructive pulmonary disease (COPD) comprises a group of pulmonary abnormalities of the airways or lung parenchyma, bronchitis or emphysema and is a major cause of morbidity and death throughout the world (Petty 2006; Huertas & Palange 2011). In addition to these pulmonary abnormalities, COPD is associated with significant effects in distant organs outside the lungs (Agustí *et al.* 2003; Gan *et al.* 2004). Peripheral skeletal muscle dysfunction is characterized by reduced muscle strength and endurance and considered one of the main systemic effects of emphysema (Couillard & Prefaut 2005; Swallow *et al.* 2007). Therefore, it is important to understand how muscle function is affected, and to identify the factors that contribute to the muscle dysfunction, and to identify the mechanism of muscle wasting in COPD so as to improve the management of the disease (Wüst & Degens 2007). The literature contains numerous animal models that develop emphysema, resulting in destruction of lung parenchyma structure with morphological and histological alterations equivalent to those in humans (Mahadeva & Shapiro 2002; Wright & Churg 2002).

Experimental models using proteolytic enzymes such as papain or elastase, instilled into the airways of animals, are based on unbalanced protective and aggressive substances in pulmonary tissue (Fusco *et al.* 2002; Antunes & Rocco 2011). In general, animal models present advantages such as homogeneity, usually good reproducibility, no difference with different therapies and a wide range of unpredictable factors affecting the development of the disease in clinical conditions (Holecek 2012). As the prevalence of cachexia in patients with COPD is up to 45% (Schols *et al.* 1993), its aetiology in the disease is multifactorial, and the number of papers examining muscle loss in models of COPD is extremely small, it would be beneficial if animal models could reproduce the human cachectic disorders as closely as possible. Mattson *et al.* (2004) demonstrated that emphysema induces fibre atrophy and the response is not specific to locomotory muscles composed of a given fibre-type or oxidative capacity, in hamsters after 180 days of pulmonary emphysema induced by elastase instillation (25 IU/100 g body weight). Rinaldi *et al.* (2012) described muscular changes and dysfunction, particularly in muscles with a mixed fibre-type composition, on an experimental model of six months of cigarette smoke exposure, and showed that this model led to systemic problems resembling those seen in humans with emphysema. In addition, Tonon *et al.* (2013) demonstrated that muscle atrophy, observed in a model of 60 days of emphysema induced by papain instillation (40 mg/ml) in rats, is mediated by increased muscle proteolysis, with involvement of oxidative stress.

Oxidative stress, resulting from an inability of the antioxidant systems to cope with elevated oxidant production, plays an important role in altering peripheral muscle function in patients with COPD (Zhang *et al.* 2010). Skeletal muscle is a highly malleable tissue that responds to changes in its pattern of activity or the mechanical and environmental stresses placed upon it. The signalling pathways involved in these multiple adaptations have been described. Reactive oxygen species are produced at various sites in skeletal muscle, and there is increasing evidence that these species play targeted roles in modulating redox-sensitive signalling pathways that are important to the muscle for making adaptations (Jackson 2009; Powers *et al.* 2010). The oxidative modifications induced by oxidants on key muscle proteins involved in muscle structure, metabolism and contraction of experimental models of disease have a great impact on their function, structure and protein balance, leading to degradation and consequent atrophy (Powers *et al.* 2010; Barreiro 2014).

Our study was motivated by three observations which emerge from the previous literature:

(1). Different changes are observed at different experimental times in different experimental models of emphysema.

(2). Redox and proteolytic modifications can be considered representative of skeletal muscle loss as a systemic manifestation of the disease.

(3). Thus far, no studies have compared oxidative stress, muscle mass loss and muscle adaptation in different models of pulmonary emphysema.

In order to explore these three poins in this study, we have investigated whether emphysema induced by elastase or papain triggers the same systemic effects on skeletal muscle and how this might be related to oxidative stress and proteolysis.

Materials and methods

Animals

Adult male Syrian Golden hamsters, weighing 100–140 g, were used (n = 10/group). The animals were given water and commercial food (Nuvilab CR1; Nuvital Nutrients Ltd, Colombo, PR, Brazil) *ad libitum*, and the environment was controlled on a 12-h light/dark cycle.

The protocols conformed to the Guide for the Care and Use of Laboratory Animals [DHEW Publication No. (NIH) 86–23, Revised 1985, Office of Science and Health Reports, DRR/NIH, Bethesda, MD 20892], and the study was approved by the Ethics Committee on Animal Experimentation from the Universidade Estadual de Londrina, Brazil (ref. 8288).

The animals were randomly divided into three groups, according to the instillation procedure used to induce emphysema. Under deep ketamine/xylazine anaesthesia (150/30 mg/kg i.m.), saline (0.3 ml/100 g body weight; control + saline [CS] group); papain (40 mg/100 g body weight in 0.3 ml normal saline) emphysema with papain [EP] group) (Tonon *et al.* 2013) or porcine elastase (5.2 IU/100 g body weight [Alfa Aesar, Shrewsbury, MA, USA] in 0.3 mL normal saline) emphysema with porcine elastase [EE] group) (Hayes *et al.* 1975) were instilled intratracheally through a 27-gauge hypodermic needle, according to the procedure described by Mattson *et al.* (2002b) with modifications. The procedure involves making a short incision in the skin of the tracheal region, seclusion of the muscle layer and trachea, insertion of the needle between tracheal rings, instillation and final suturing of the skin. To ensure a uniform distribution of saline, elastase or papain throughout the lungs, each animal was submitted to a gentle manual negative pressure manoeuvre. Briefly, just after instillation, in the moment of final expiration, the thorax was momentarily restrained to prevent lung expansion. After active inspiration, a negative pressure is generated and the thorax released. This manoeuvre, through acute differences of pressure, allows complete spread of the instilled solution to the distal airways.

After the procedure, the animals were returned to their cages. Their appearance and body weights were monitored daily for the first two weeks and then once a week for 70 days (Tonon *et al.* 2013). The cachexia index was determined {[(initial body mass − final body mass + body mass gain of control)/(initial body mass + body mass gain of control)] × 100%}, considering the initial and final body weight of the emphysemic animals and body weight gain in the CS group to identify a pattern of general wasting. (Guarnier *et al.* 2010). This index reflects both loss of total body weight and absence of weight gain (Tonon *et al.* 2013).

Ethical approval

The experimental design and protocols were approved by Ethic in Animal Experimentation Committee from Universidade Estadual de Londrina (register n. 19011201362).

Tissue collection and preparation

Seventy days after intratracheal instillation, the hamsters were weighed and euthanized. The right gastrocnemius muscle was excised, weighed, frozen in liquid nitrogen and stored at −86°C until use for analysis of oxidative parameters. The left gastrocnemius was divided: one portion was saved for morphometric histological procedures, and the other portion was pulverized, frozen in liquid nitrogen and stored at −86°C until used for proteolysis assays.The gastrocnemius muscle has previously been demonstrated as a good indicator of alterations in the skeletal muscle of emphysemic hamsters (Mattson *et al.* 2004), including in aspects related to oxidative parameters (Mattson *et al.* 2002b; Tonon *et al.* 2013). In hamsters there is no gross division of fibres in this muscle (Mattson *et al.* 2002a), and therefore, the whole muscle, and consequently both fibre types, is typically analysed. In addition, the middle lobe of the right lung was fixed in 10% formalin for morphometric evaluation.

For the oxidative stress analysis, muscles from CS, EP and EE hamsters were prepared as described above. Tissues were placed on ice and homogenized for 60 s periods at 60 s intervals in an Ultraturrax homogenizer containing 10 mg/ml, 50 mg/ml or 60 mg/ml tissue in 50 mM or 10 mM KH_2PO_4/K_2HPO_4 buffer and 120 mM KCl at pH 7.4. The total homogenate (10 mg/ml) was used for the tert-butyl hydroperoxide-stimulated chemiluminescence and thiobarbituric acid-reactive substances (TBARS) assays. For total protein carbonylation determination, tissues (60 mg/ml) were treated according to the method of Reznick and Packer (1994), with adaptations as described below. For total and oxidized glutathione assays, the supernatant from total homogenate was obtained by centrifugation at 10,000 × ***g*** for 15 min at 4°C from a homogenate 50 mg/ml.

Morphometric analysis of lungs and gastrocnemius

After the middle lobe of the right lung had been removed, samples were fixed in paraformaldehyde for 48 h and embedded in paraffin for histological studies. Paraffin-embedded tissues were semiserially sectioned into cuts of 5 μm (5 cuts/slide per lung, interval of 50 μm/cut). After this procedure, cuts were stained with haematoxylin and eosin.

To verify emphysema establishment and severity, alveolar destruction was determined by the number of times that a predetermined group of coherent lines (1.25 mm^2 area and 1.50 mm total length) crossed the parenchymal structures. The group identifications were covered, and lung images were captured (three non-coincident fields/section) using an optical microscope (100 × magnification). Images were obtained using a high-resolution camera coupled to the microscope. The base lines were then superposed on to the images; the less the structures were crossed, the more extensive was the lesion (adapted from Fusco *et al.* 2002). Additionally, to verify whether the number of captured fields was enough, a coefficient of variation was calculated, with acceptable values being below 20%. All sets of measurements by animal were considered acceptable. The mean of the 30 values from each animal was calculated. These values, named the crossed alveolar intercepts (CAI), were used to represent each animal in the group comparison.

To establish a histological parameter of muscle adaptation, the cross-sectional area of gastrocnemius fibres was measured. Muscle samples were collected and fixed in methanol and glacial acetic acid (3:1 v/v) for 70 min and then embedded in paraffin. Semiserial sections of 5 μm were made (5 cuts/slide, interval of 50 μm/cut) from each muscle. The sections were stained with haematoxylin and eosin. To measure the cross-sectional area, the slide identifications were covered, and muscle images were captured (5 fields/cut per animal), totalling approximately 600 measured fibres/animal, using an optical microscope (200 × magnification). Images were obtained using a high-resolution camera coupled to the microscope. An image analysis system (Image-Pro-Plus 4.0; Media Cybernetics, Silver Spring, MD, USA) was used to determine fibre area in square micrometres. Because of natural heterogeneity in the fibre size distribution within the groups, the values were grouped by procedure (CS, EE or EP), and the frequency distribution was estimated based on area intervals (30 classes) from 600 to 15000 μm^2.

Oxidative stress parameters

Thiobarbituric acid-reactive substances (TBARS) assay. Lipid peroxidation is a direct consequence of oxidative stress in tissues. The chain reaction produces malondialdehyde (MDA), which can form adducts modifying protein structures. Thus, the extent of lipid peroxidation of the muscle homogenates from each group was determined by the TBARS assay. MDA formed during peroxidation reacts with thiobarbituric acid (TBA) to generate a coloured product, a $(TBA)_2$–MDA adduct. In an acid solution, $(TBA)_2$–MDA absorbs light at 532 nm and is readily extractable by an organic solvent such as n-butanol. MDA levels were measured, and the results were expressed in nanomoles per gram of tissue (Oliveira & Cecchini 2000).

Carbonyl protein content. Carbonyl proteins are a modification caused by exposure of proteins to oxidative stress. The carbonyl protein content was measured as described by Reznick and Packer (1994), with modifications. Gastrocnemius muscle (60 mg/ml) was placed in glass homogenization tubes containing homogenizing buffer (50 mM phosphate buffer, 1 mM ethylenediamine tetraacetic acid, pH 7.4). The tissue samples were homogenized and incubated for 15 min in an ice bath. The samples were centrifuged at 3000 × ***g***

for 10 min at room temperature, and 1 ml of each protein extract was placed in a glass tube. A volume of 4 ml 2,4-dinitrophenylhydrazine (DNPH) solution prepared in 2.5 N HCl was added to each tube, and the reaction mixtures were incubated for 1 h at room temperature, with vortexing every 15 min. Next, the samples were washed with 5 ml 20% trichloroacetic acid (TCA) (w/v) and centrifuged for 10 min to collect the protein precipitates. Another wash was performed using 10% TCA, and the protein pellets were dispersed mechanically. Finally, the pellets were washed three times with 4 mL ethanol–ethylacetate (1:1, v/v) to remove free DNPH and lipid contaminants. The final precipitates were dissolved in 2 ml 6 M guanidine hydrochloride, and any insoluble materials were removed by additional centrifugation. The carbonyl content was calculated by comparing the peak absorbance at 355–390 nm of the DNPH-treated samples with that of samples treated with only 2.5 M HCl. The following formula was used to calculate the concentration of carbonyls: C = Abs (355–390 nm) × 45.45 nmol/ml, where C is the concentration of DNPH per millilitre, and 45.45 is its absorption coefficient. The procedures were performed in an ice bath until the TCA wash step. The carbonyl content was expressed as nanomoles per milligram of total protein.

Tert-butyl hydroperoxide-initiated chemiluminescence. The tert-butyl hydroperoxide-initiated chemiluminescence assay was used to analyse the levels of lipid hydroperoxides in muscle homogenate of animals. In this assay, an increase in chemiluminescence is closely related to the oxidative stress previously suffered by the tissue. The assay induces the consumption of antioxidants and augments the formation of lipid hydroperoxides, which results in increased photon emission (Oliveira & Cecchini 2000; Barbosa *et al.* 2003; Mattson & Martin 2005).

Reaction mixtures in 2-ml luminescence tubes consisted of total muscle homogenate (8.75 mg/ml), 10 mM KH_2PO_4/K_2HPO_4 buffer (with 120 mM KCl, pH 7.4) and 6 mM tert-butyl hydroperoxide, in a final volume of 1 ml. The tert-butyl hydroperoxide-initiated chemiluminescence reaction was assessed using a TD 20/20 luminometer (Turner Designs, Sunnyvale, CA, USA), with a response range of 300–650 nm. The tubes were kept in the dark until the assay was carried out in a room at 33 ± 1°C (Gonzalez-Flecha *et al.* 1991; Oliveira & Cecchini 2000). For each animal, a 60-min curve, in which each point represented the differential smoothing of 600 readings, was obtained by interpolation; after that, the area under the chemiluminescence curve was extracted by integral calculus of each animal curve. This value, expressed as area under the chemiluminescence curve in relative light units and corrected by gram of tissue (RLU/g tissue), together with total analysis of the chemiluminescence curve, was used to determine the amount of lipid hydroperoxides present in the sample.

Total (GST) and oxidized (GSSG) glutathiones. Redox state was determined by the levels of total (GST) and oxidized (GSSG) glutathione in homogenate supernatant, extracted as described above. The reactions were based on titration with 5,5-dithio-bis (2-nitrobenzoic acid), which results in the formation of a yellow colour. Oxidized glutathione (GSSG) was determined by previous incubation with 4-vinylpyridine for 60 min at room temperature, according to the method described by Tietze (1969). Supernatant volumes were adjusted for the assay to contain 50-mg tissue per millilitre of KH_2PO_4. The results are expressed in micromoles per milligram of protein.

Muscle proteolytic activity

Chymotrypsin-like proteolytic activity was quantified using a Proteasome Glo™ Chymotrypsin-like Cell Based Assay kit (Promega, Madison, WI, USA). This kit estimates the activity of the proteasome; the final objective is to evaluate whether proteolytic activity is present in skeletal muscle. The assay involves the use of a specific luminogenic substrate (succinyl-leucine-valine-tyrosine-aminoluciferin) to determine chymotrypsin-like activity. Proteasome cleavage of the substrate produces a luminescent signal from the luciferase contained in the reaction medium. The three major proteolytic activities (chymotrypsin-like, trypsin-like and postglutamyl peptide hydrolytic or caspase-like activity) occurring within the 20S core of the 26S proteasome complex are responsible for most of the protein degradation, which includes degradation of damaged cellular proteins. Therefore, this coupled-enzyme system, with simultaneous proteasome cleavage of substrate and luciferase consumption of the released aminoluciferin, results in a luminescent signal that can be considered proportional to the amount of proteasome activity in the muscle tissue.

For the assay, 25 mg muscle powder was added to 1 ml 10 mM KH_2PO_4, pH 7.4, in 0.9% NaCl and gently homogenized. Fifty microlitres of the resulting muscle homogenate was pipetted in duplicate on to 96-well microplates, and the final reagent mixture with luminescent substrate was added to the medium. After 5 min, under light protection, the luminescent signal at the plate was detected with a Glo-Runner microplate reader luminometer (Turner Designs), and the results were expressed as RLU per milligram total protein.

In a similar manner, the activity of a calcium-dependent protease was measured by a chemiluminescence assay using a Calpain-Glo™ Protease Assay kit (Promega). Homogenates were prepared at a concentration of 6.25 mg/ml 10 mM KH_2PO_4 buffer, pH 7.4, in 0.9% NaCl. The luminescent signal is proportional to the calcium-dependent proteolytic activity in samples, which is also based on the specific reaction of the labelled luciferin substrate by the enzyme luciferase. The results are expressed as RLU per milligram tissue.

Protein concentration

The protein concentration was determined by the method of Lowry *et al.* (1951) modified by Miller (1959). This method involved the use of bovine serum albumin (BSA) as a standard.

Statistical analysis

When the distribution was considered normal, the results are presented as mean ± standard error of the mean (SEM) for 10 animals and values were compared using one-way analysis of variance followed by Bonferroni's multiple comparison test, with $P < 0.05$ considered significant. Curves of chemiluminescence induced by tert-butyl hydroperoxide were compared by two-way ANOVA. When the distribution did not pass a normality test, data are presented as median and interquartile range, and values were compared by Kruskall–Wallis test followed by Dunn's multiple comparison test. For the muscle morphometry data, histograms of the fibre cross-sectional areas were prepared and absolute frequencies calculated.

Results

Emphysema status

The extent of lung damage in each group was evaluated by the number of CAI. A previous pilot study demonstrated no lung damage in the saline-treated group (CS) relative to a control (no saline, papain or elastase instillation – data not shown). The EE and EP groups had significantly lower CAI values (48.17 ± 1.16 and 51.56 ± 0.49, respectively) than the CS group (70.64 ± 0.58, $P < 0.0001$ in both comparisons). The EE and EP groups also had significant differences in pulmonary emphysema ($P < 0.05$). Representative images of lung injury are presented in Figure 1, and CAI values are presented in Table 1. The cachexia index, using gain of body mass in the control group as the reference, was 4.6% ± 0.48% in the EP group. The EE group did not show cachexia (0.76% ± 1.17%). In addition, general body weight showed by CS, EE and EP during the course of 70 days is demonstrated on supplemented Figure 1. The ratio of gastrocnemius mass (MM)/total mass (MT) was significantly increased in the EE (0.16 ± 0.003%) when compared to CS (0.14 ± 0.004%). In contrast, when the CS and EP groups were compared, the relationship showed a significantly decrease (0.12 ± 0.004%). These results represented 8.37% muscle gain in the EE group and 18.34% muscle loss in the EP group compared with the gastrocnemius muscle weight of the CS animals.

The frequency distribution of fibre cross-sectional areas showed differences between groups. Representative images of gastrocnemius muscles are presented in Figure 2. The 50th percentile of fibre area occurred in the fourth class (2000–2499 μm^2) for the CS group, the fifth class (2500–2999 μm^2) for the EE group and the third class (1500–

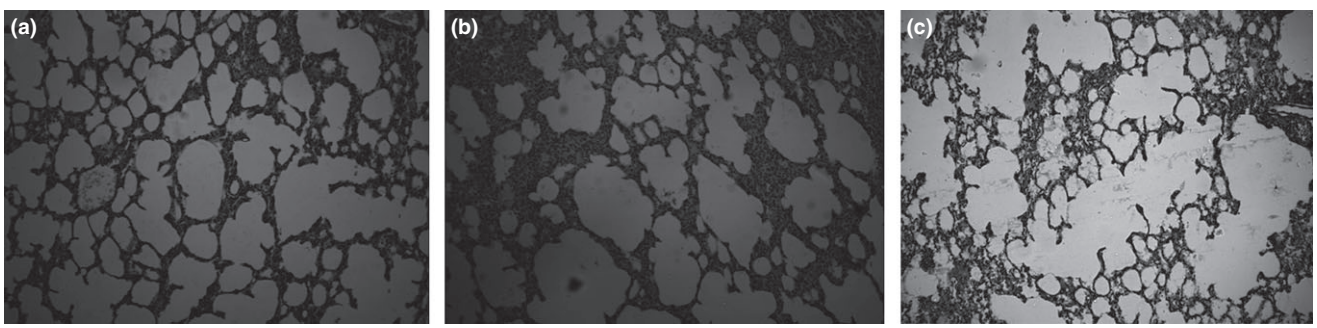

Figure 1 Histological images from lungs of hamsters treated with elastase, papain or saline. (a) control + saline (CS): animals treated with 0.3 ml sterile saline only; (b) emphysema + elastase (EE): animals treated with 0.3 ml 5.2 IU elastase in sterile saline; and (c) emphysema + papain (EP): animals treated with 0.3 ml 40 mg/ml papain in sterile saline. Alveolar destruction was determined by the number of times that a predetermined group of coherent lines (1.25 mm^2 total area and 1.50 mm total length) crossed the parenchymal structures, named crossed alveolar intercepts. The less these structures are crossed, the more extensive is the lesion.

Table 1 Animal and skeletal muscle adaptation characteristics

	CS	EE	EP
Crossed alveolar intercept	70.64 ± 0.58	48.17 ± 1.16*	51.56 ± 0.49*†
Cachexia index (%)	–	0.76 ± 1.17	4.6 ± 0.48
MM/MT (%)	0.14 ± 0.004	0.16 ± 0.003*	0.12 ± 0.004*†
% of variation on gastrocnemius (compared with CS)	–	+8.37	−18.34

CS – Group instilled with 300 μl NaCl 0.9%; EE – Group instilled with 300 μl papain 40 mg/ml in NaCl 0.9%; EP – Group instilled with 300 μl elastase 5.2 IU in NaCl 0.9%. Cachexia index = (initial body weight − final body weight + body mass gain of CS group)/(initial body weight − body mass gain of CS group) × 100 (Tonon *et al.* 2013). MM – gastrocnemius weight; MT – Total animal weight; MM/MT – ratio between values × 100, expressed as percentage. Values are expressed as means ± SEM (CS: $n = 10$; EE: $n = 10$; EP: $n = 10$). *$P < 0.05$ compared with CS and †$P < 0.05$ comparing EP with EE by one-way ANOVA followed by Bonferroni's multiple comparison test.

Table 2 Effect of emphysema on skeletal muscle in terms of TBARS, GST, GSSG in hamsters

	CS	EE	EP
TBARS (nmol/g tissue)	0.42 [0.35–0.67]	0.49 [0.41–0.59]	0.42 [0.28–0.49]
GST (μM/mg total proteins)	73.5 [67.13–83.7]	82.1 [65.83–86.26]	62.15 [50.07–70.68*
GSSG (μM/mg total proteins)	6.15 [5.6–7.78]	6.82 [2.75–7.65]	4.13 [2.42–5.85]

CS – Group instilled with 300 μl NaCl 0.9%; EE – Group instilled with 300 μl papain 40 mg/ml in NaCl 0.9%; EP – Group instilled with 300 μl elastase 5.2 IU in NaCl 0.9%. TBARS – thiobarbituric acid-reactive substances. GST – total glutathione. GSSH – oxidized glutathione. Values are expressed as median [25–75 percentile]. Groups were composed of 10 animals. *$P < 0.05$ when EP with EE were compared by Kruskall–Wallis test followed by Dunn's multiple comparison test.

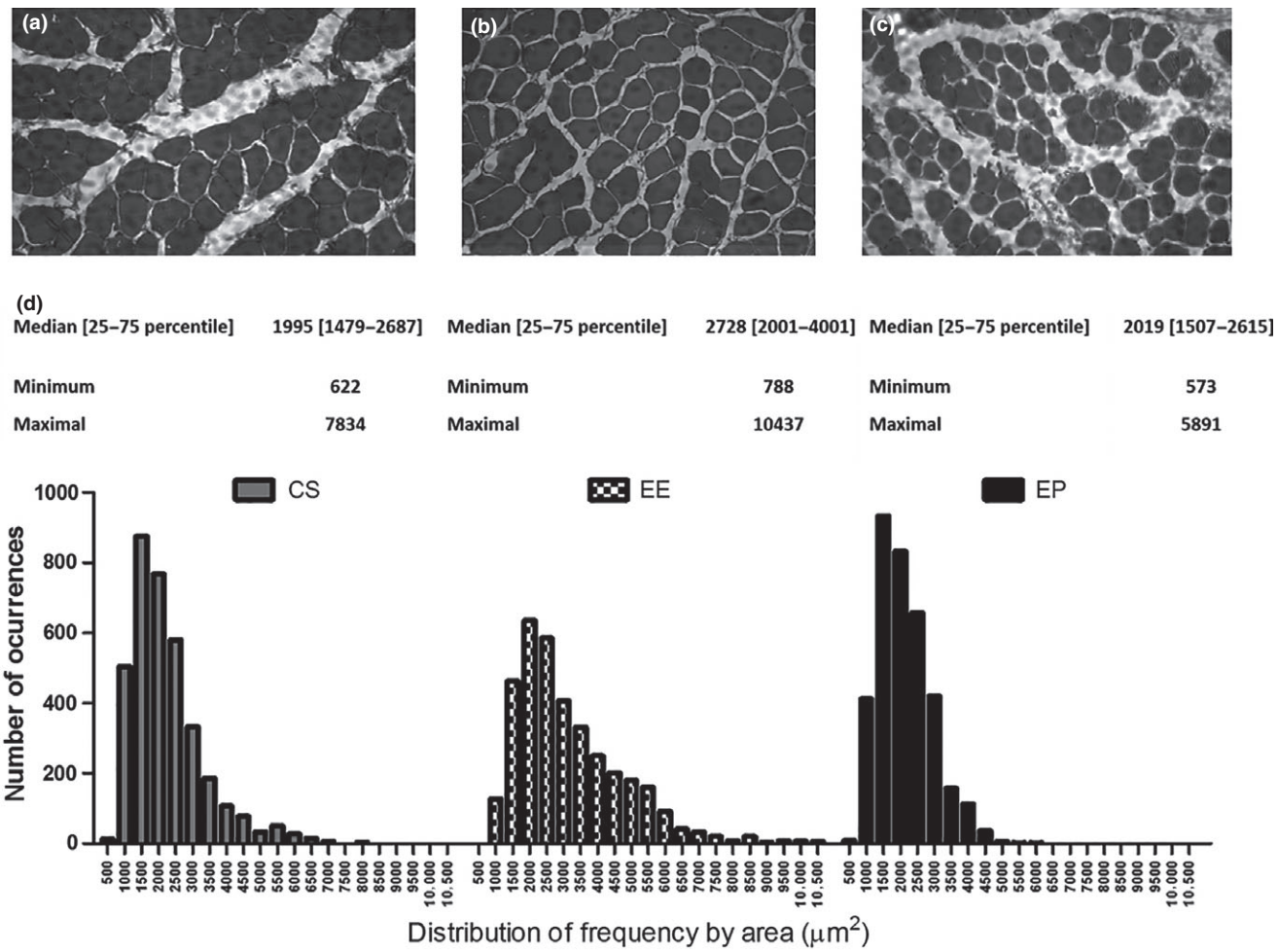

Figure 2 Histological and morphometric differences in skeletal muscles of hamsters with emphysema induced by papain or elastase. (a) control + saline (CS): animals treated with 0.3 ml sterile saline only; (b) emphysema + elastase (EE): animals treated with 0.3 ml 5.2 IU elastase in sterile saline; and (c) emphysema + papain (EP): animals treated with 0.3 ml 40 mg/ml papain in sterile saline. Animals were euthanized after 70 days and lungs stained with haematoxylin and eosin. Original magnification 200 × . (d) Histogram of frequency distribution of fibre cross-sectional areas (μm^2). Muscles were sectioned, and five semiserial cuts per slide (50-μm interval) were positioned on two slides. Three fields per cut were captured and 20 fibres measured per field per animal, totalling 600 fibre measurements per animal. The values were grouped by procedure (CS, EE or EP) and frequency distribution determined. Values of median [25–75 percentiles], minimal and maximal values were inserted in the graph to illustrate changes in the distribution between groups.

1999 μm^2) for the EP group. The cumulative frequency to the class containing the 50th percentile was 1401 occurrences in the CS group, compared with 1811 occurrences for the EE group, and 2195 for the EP group. The complete histograms of the frequency distributions are presented in Figure 2(d).

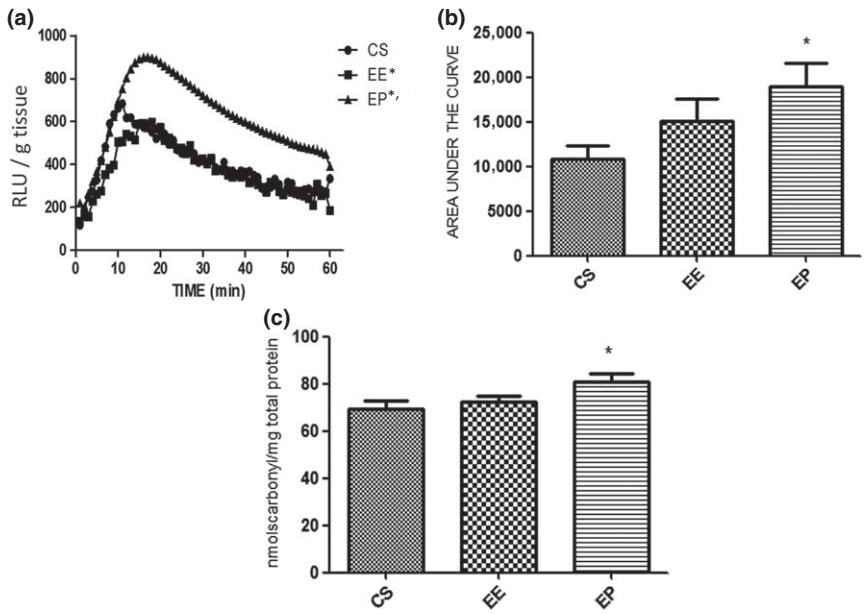

Figure 3 Effect of emphysema induced by papain or elastase on skeletal muscle of hamsters in terms of lipid hydroperoxide and carbonyl proteins. (a) The tert-butyl hydroperoxide-initiated chemiluminescence was monitored continuously for 60 min in gastrocnemius homogenates. Each curve represents the mean of 10 animals' curves, corrected by grams of tissue. The entire curves were used to perform statistical comparison by two-way ANOVA. (b) Area under the curve of each animal curve was determined to compare groups. (c) Levels of protein carbonylation in muscle homogenates of control, emphysema induced by elastase and emphysema induced by papain animals. The difference was assessed by one-way ANOVA followed by Bonferroni's multiple comparison test. Values are expressed as means ± SEM (n = 10 per group).*$P < 0.05$ compared with CS and $^{\#}P < 0.05$ comparing EP with EE.

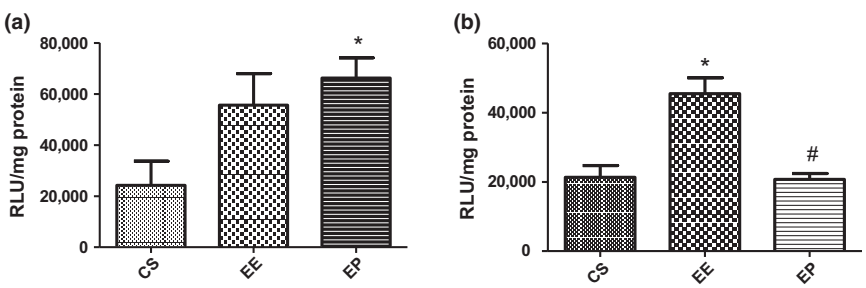

Figure 4 Quantification of proteolytic activity in gastrocnemius of hamsters with emphysema induced by papain or elastase quantified by a luminescent kit. (a) Chymotrypsin-like activity (b) Calpain-like activity. Control and experimental groups were compared by one-way ANOVA followed by Bonferroni's test. *$P < 0.05$ compared with CS. $^{\#}P < 0.05$ compared with EE. CS – Group instilled with 300 μl NaCl 0.9%; EE – Group instilled with 300 μl papain 40 mg/ml in NaCl 0.9%; EP – Group instilled with 300 μl elastase 5.2 IU in NaCl 0.9%.

Oxidative stress

Figure 3(a) presents chemiluminescence curves from the CS, EE and EP groups at 60 min, obtained by interpolation. The two-way ANOVA showed significant differences in all comparisons (CS × EE, CS × EP and EE × EP, $P < 0.05$). The area under the chemiluminescence curve, obtained by interpolation, was significantly higher in the EP group (18960 ± 2598 RLU/g tissue) compared with the CS group (10775 ± 1564 RLU/g tissue, $P < 0.05$), but the EE group (15106 ± 2469 RLU/g tissue) was not significantly different.

Figure 3(c) shows carbonyl protein levels in the CS, EE and EP groups. Only the EP group (80.71 ± 3.39 nmol carbonyl/mg total proteins) showed higher carbonyl protein levels relative to the CS group (69.16 ± 3.55 nmol carbonyl/mg total proteins, $P < 0.05$).

TBARS and GSSG did not show any significant differences between the groups. GST levels were not significantly different between the CS group (median, 73.5 [IQR, 67.13–83.7] μM/mg total proteins) and the EP group (median, 62.15 [IQR, 50.07–70.68] μM/mg total proteins) or the EE group (median, 82.10 [IQR, 65.83–86.26] μM/mg total

proteins). However, the GST level in the EP group was significantly lower than in the EE group ($P < 0.05$). These data are presented on Table 2.

Analyses of chymotrypsin and calpain-like proteolytic activities

Chymotrypsin-like proteolytic activity did not differ between the CS group (24259 ± 9445 RLU/mg protein) and the EE group (55665 ± 12299 RLU/mg tissue). However, the EP group (66265 ± 7905 RLU/mg protein) had a significantly higher chymotrypsin-like proteolytic activity (Figure 4a). On the other hand, calpain-like activity was significantly higher in the EE group (45490 ± 4585 RLU/mg total protein) than the CS group (21330 ± 3382 RLU/mg total protein) and the EP group (20735 ± 1668 RLU/mg total protein), but the CS and EP groups did not differ (Figure 4b).

Discussion

Emphysema has been shown to reduce the contractile function of locomotory skeletal muscle (Bernard *et al.* 1998) and leads to skeletal muscle loss in humans (Gosselink *et al.* 1996). These processes have been credited to muscle mass adapting to modified oxygen uptake and distribution (Wüst & Degens 2007). In addition, oxidative stress is involved in the process of skeletal muscle changes in patients with COPD (Fermoselle *et al.* 2011). However, as gaining access to human biopsy samples for experiments is difficult, most studies regarding molecular and biochemical aspects of COPD use animals, with different ways of inducing emphysema. Most experimental models use proteolytic enzymes, such as papain and elastase, instilled or nebulized into the airways. These models are based on theory regarding the unbalanced production of aggressive and protective substances in the lung (Fusco *et al.* 2002). They result in histological, morphological and physiological alterations to the lungs equivalent to the changes found in human emphysema (Hayes *et al.* 1975). In addition, few studies consider the influence of time used for induction, or differences in methods of inductions, on systemic manifestations.

In the present study, both elastase and papain caused pulmonary injury at a level sufficient to promote emphysema. Papain and elastase produced a pattern of panacinar emphysema with part of the lobe histoarchitecture preserved, but rupture of the alveolar septs. However, injuries in the ruptured extremities were more extensive with elastase compared with papain induction. In addition, quantitative evaluation of emphysema showed a significant decrease in the CAI values compared with saline instillation. The induction doses used were very close to the doses that increase animal mortality immediately after induction; despite this, CAI were different between the groups. Classic studies in the literature compared the two models (Karlinski & Snider 1978; Schulz *et al.* 1989) and demonstrated that, although they induce slightly different patterns of lesion, they both establish the histological and functional characteristics of emphysema. However, at present, no studies have demonstrated differences in the skeletal muscle adaptations between the two models.

In emphysema, the main factors that contribute to muscle wasting dysfunction are muscle weakness and loss of muscle mass (Wüst & Degens 2007), which both have a direct impact on exercise tolerance. In the present study, when systemic adaptation was evaluated by general and skeletal muscle losses, gross morphological and morphometric differences were found between the two forms of induction. The gastrocnemius muscle has previously been demonstrated as a good indicator of alterations in the skeletal muscle of emphysemic hamsters, where there is no obvious gross division of fibres and consequently, the total muscle is analysed (Tonon *et al.* 2013).

In the present study, elastase induction did not promote general loss, unlike in the papain group, which showed 4.6% weight loss compared with control group 70 days after induction. These data were reflected in skeletal muscle loss and in morphometry to some extent. In principle, these data could be explained by differences in food restriction caused by hypoxia. Some studies reported the action of nicotine in modulating leptin secretion and consequently appetite. This pathway obviously reflects the influence of hypoxia and thus seems to be particularly important in cigarette smoke-induced emphysema. Decrease in oxygen consumption and increase in cytokine levels are present in the very early stages after experimental emphysema induction and have their origin in the pulmonary lesion. We monitored plasma TNF-alpha levels at 10, 20, 40 and 70 days after instillation and found no significant differences between CS, EE and EP groups (data not shown). In addition, we monitored food consumption during the first 15 days after induction and also found no differences between groups although the surgery procedure could affect swallow. Although the anorexic effects of hypoxia may contribute to muscle wasting as well, reductions in muscle mass independent of hypophagia have also been reported (Langen *et al.* 2013).

Studies in humans and animals have shown that skeletal muscle in COPD demonstrates increased oxidative stress parameters, which could have a relationship with hypoxia through increased generation of superoxide anion in the respiratory electric chain (Mattson *et al.* 2002b). Mattson *et al.* (2002a) found that fibre cross-sectional area and distribution also varied within and among muscles in their studies of hamsters with emphysema induced by elastase. This information is reinforced by correlation with citrate synthase activity, a marker of muscle oxidative capacity. However, based on our results, models of inducing emphysema by elastase or papain seem to promote different systemic consequences at the same time point.

The difference in the distribution of fibre cross-sectional area in this study showed that papain induction can produce at least initial skeletal muscle adaptation at 70 days after induction. Although no fibre type was assayed, it is reasonable to assume that fibre type modification would be present, as observed in previous studies. Together, these data

indicate that skeletal muscle adaptation is different between the two models.

Among several factors, oxidative stress is a major component in the aetiology of skeletal muscle dysfunction. Although low levels of oxidants are required for normal cell adaptation (Fermoselle et al. 2011), moderate to high levels of reactive oxygen species alter the function and structure of proteins (Grune *et al.* 2003). Langen *et al.* (2013) point to oxidative stress as an important key factor in proteolysis regulation affecting the atrophy associated with COPD. Specifically, protein carbonylation, a common variety of protein oxidation, alters the function of key enzymes and structural proteins involved in muscle contraction (Fermoselle *et al.* 2011; Tonon *et al.* 2013). Thus, it is reasonable to evaluate whether both emphysema models developed oxidative modifications, as other studies have shown that MDA is elevated in skeletal muscle of humans with COPD, in hamsters 180 days after induction and in mice 34 weeks after induction of emphysema with elastase (Mattson *et al.* 2002b; Wijnhoven *et al.* 2006; Fermoselle *et al.* 2011). In this study, TBARS, the classic method for evaluating oxidative stress, showed no difference between groups. In contrast, when chemiluminescence stimulated by t-BOOH was assayed, the gastrocnemius muscle of animals with emphysema induced by papain showed higher membrane lipid peroxides. Chemiluminescence is a very sensitive method that takes into account the kinetic analysis of the ascending part of the curve in addition to its peak. The technique is based on the concept that increased variation in these two parts of the curve represents higher levels of pre-existing membrane lipoperoxides. Thus, when a tissue is challenged with tert-butyl hydroperoxide, the chemiluminescence curves should reflect both the attack suffered by the membrane and the tissue antioxidant consumption mediating the damage caused by this attack. Thus, the change in membrane permeability due to oxidative imbalance can be observed based on the analysis of the chemiluminescence curve and confirmed through the area under the chemiluminescence curve (Barbosa *et al.* 2003). In addition, MDA can react with proteins leading to carbonylation (Guarnier *et al.* 2010), which could diminish its adducts at the time point of this study. Here, the EP group showed an increase in the overall height of the chemiluminescence curve in both experimental periods, with a maximum height achieved. This result was in agreement with the peak of carbonyl proteins content and area under the chemiluminescence curve. Yet, muscles from hamsters with emphysema induced by papain showed decreased GST compared to elastase, a parameter of redox balance that is frequently diminished in skeletal muscle atrophy, with no increasing in GSSG levels (Guarnier *et al.* 2010; Bernardes *et al.* 2014). Perhaps the thiolation group or tripeptide may have other destinations, such as thiolation or glutathiolation. As we have evidence to support this conclusion, we propose that the ratio GST/GSSG may not reliably reflect the redox status when muscle loss occurs at least in models of emphysema. But the evaluated parameters still lead to the conclusion that skeletal muscle adaptation differs between elastase and papain induction, including events related to oxidative stress.

Oxidative stress may differentially regulate protein loss within peripheral muscles of in patients with severe COPD who exhibit different body composition (Fermoselle *et al.* 2012). This seems to be the trigger factor to the muscle mass loss. A model that is unable to generate oxidative stress in the muscle does not trigger skeletal muscle loss. As far as we are aware from the previous literature, the only model that demonstrated muscle loss in papain-induced emphysema was the study published by Tonon *et al.* (2013), which showed increased chymotrypsin-like activity in the skeletal muscle of hamsters with emphysema 60 days after induction. No studies involving elastase-induced emphysema were performed in this context. Fermoselle *et al.* (2011) demonstrated induction of several components of atrophy pathways in the elastase induction model after 34 weeks. Interestingly, no studies had evaluated calpain or calpain-like activity. Proteasome and calpains are two of the four proteolytic systems in skeletal muscle. They are extensively involved in metabolic protein turnover and have different effects on atrophy processes (Goll *et al.* 2007). The proteasome is involved in and has its activity induced by oxidative stress (Powers *et al.* 2010). It can accelerate degradation of oxidatively modified proteins, leading to atrophy (Grune *et al.* 2003). The calpains seem to be involved in turnover of myofibrillar proteins (Goll *et al.* 2007). When activated, calpains can degrade myofilament stabilizers, exposing heavy- or light-chain myosin to degradation by proteasome (Costelli *et al.* 2005). We can speculate that this may be made a possible explanation as evidenced by the changes in fibre size demonstrated in the EE group, which showed a concomitant increase in calpain-like activity.

In summary, elastase and papain can induce pulmonary emphysema through practically the same extension of pulmonary lesions. However, by 70 days after emphysema induction, the papain model of induction led to skeletal muscle atrophy and oxidative stress activation concomitant to chymotrypsin-like proteolytic activity; elastase induction led to increased muscle weight and fibres of higher sizes concomitant to calpain-like activity participation in the adaptation. These data, when put together, indicate that elastase and papain, when used to induce experimental models of emphysema, lead to different types of adaptation. These findings provide more information for choosing a suitable experimental model when studying skeletal muscle adaptations to emphysema.

Conflict of interest

The authors declare no conflict of interest.

Funding source

This research was supplied by Coordenação de Pessoal de Nível Superior (CAPES) and Fundação Araucária (FA - PR, Brazil).

References

Agustí A.G.N., Noguera A., Sauleda J., Sala E., Pons J. & Busquets X. (2003) Systemic effects of chronic obstructive pulmonary disease. *Eur. Respir. J.* **21**, 347–360.

Antunes M.A. & Rocco P.R. (2011) Elastase-induced pulmonary emphysema: insights from experimental models. *An. Acad. Bras. Ciênc.* **83**, 1385–1396.

Barbosa D.S., Cecchini R., El Kadri M.Z., Rodriguez M.A., Burini R.C. & Dichi I. (2003) Decreased oxidative stress in patients with ulcerative colitis supplemented with fish oil omega-3 fatty acids. *Nutrition* **19**, 1–83.

Barreiro E. (2014) Protein carbonylation and muscle function in copd and other conditions. *Mass Spectrom. Rev.* **33**, 219–236.

Bernard S., Le Blanc P., Whittona F. *et al.* (1998) Peripheral muscle weakness in patients with chronic obstructive pulmonary disease. *Am. J. Respir. Crit. Care Med.* **158**, 629–634.

Bernardes S.S., Guarnier F.A., Marinello P.C. *et al.* (2014) Reactive oxygen species play a role in muscle wasting during thyrotoxicosis. **357**, 803–814.

Costelli P., Reffo P., Penna F., Autelli R., Bonelli G. & Baccino F.M. (2005) Ca (2 +)-dependent proteolysis in muscle wasting. *Int. J. Biochem. Cell Biol.* **37**, 2134–2146.

Couillard A. & Prefaut C. (2005) From muscle disuse to myopathy in COPD: potential contribution of oxidative stress. *Eur. Respir. J.* **26**, 703–719.

Fermoselle C., Sanchez F. & Barreiro E. (2011) Reduction of muscle mass mediated by myostatin in an experimental model of pulmonary emphysema. *Arch. Bronconeumol.* **47**, 590–598.

Fermoselle C., Rabinovich R., Ausín P. *et al.* (2012) Does oxidative stress modulate limb muscle atrophy in severe COPD patients? *Eur. Respir. J.* **40**, 851–862.

Fusco L.B., Pego-Fernandes P.M., Xavier A.M. *et al.* (2002) Modelo experimental de enfisema pulmonar em ratos induzidos por papaína. *J. Pneumol.* **28**, 1–7.

Gan W.Q., Man S.F.P., Senthilselvan A. & Sin D.D. (2004) Association between chronic obstructive pulmonary disease and systemic inflammation: asystematic review and a meta-analysis. *Thorax* **59**, 574–580.

Goll D.E., Neti G., Mares S.W. & Thompson V.F. (2007) Myofibrillar protein turnover: the proteasome and the calpains. *J. Anim. Sci.* **86**, 19–35.

Gonzalez-Flecha B., Llesuy S. & Boveris A. (1991) Hydroperoxide initiated chemiluminescence: an assay for oxidative stress in biopsies of heart, liver and muscle. *Free Radic. Biol. Med.* **10**, 93–100.

Gosselink R., Troosters T. & Decramer M. (1996) Peripheral muscle weakness contributes to exercise limitation in COPD. *Am. J. Respir. Crit. Care Med.* **153**, 976–980.

Grune T., Merker K., Sandig G. & Davies K.J. (2003) Seective degradation of oxidativey modified protein by proteasome. *Biochem Biophys Res Commun.* **305**, 709–718.

Guarnier F.A., Cecchini A.L., Suzukawa A.A. *et al.* (2010) Time course of skeletal muscle loss and oxidative stress in rats with Walker 256 solid tumor. *Muscle Nerve* **42**, 950–958.

Hayes J.A., Korthy A. & Snider G.L. (1975) The pathology of elastase-induced panacinar emphysema in hamsters. *J. Pathol.* **117**, 1–14.

Holecek M. (2012) Muscle wasting in animal models of severe illness. *Int. J. Exp. Pathol.* **93**, 157–171.

Huertas A. & Palange P. (2011) COPD: a multifactorial systemic disease. *Ther. Adv. Respir. Dis.* **5**, 217–224.

Jackson M.J. (2009) Redox regulation of adaptive responses in skeletal muscle to contractile activity. *Free Radic. Biol. Med.* **47**, 1267–1275.

Karlinski J.B. & Snider G.L. (1978) Animal models of emphysema. *Am. Rev. Respir. Dis.* **117**, 1109–1133.

Langen R.D.J., Gosker H.R., Remels A.H.V. & Schols A.M.W.J. (2013) Triggers and mechanisms of skeletal muscle wasting in chronic obstructive pulmonary disease. *Int. J. Biochem. Cell Biol.* **45**, 2245–2256.

Lowry O.H., Rosenbrough N.J., Farr A.L. & Randall R.J. (1951) Protein measurement with the folin phenol reagent. *J. Biol. Chem.* **193**, 265–275.

Mahadeva R. & Shapiro S.D. (2002) Chronic obstructive pulmonary disease: experimental animal models of pulmonary emphysema. *Thorax* **57**, 908–914.

Mattson J.P. & Martin J.C. (2005) Emphysema-induced reductions in locomotory skeletal muscle contractile function. *Exp. Physiol.* **90**, 519–525.

Mattson J.P., Miller T.A., Poole D.C. & Delp M.D. (2002a) Fiber composition and oxidative capacity of hamster skeletal muscle. *J. Histochem. Cytochem.* **50**, 1685–1692.

Mattson J.P., Sun J., Murray D.M. & Poole D.C. (2002b) Lipid peroxidation in the skeletal muscle of hamsters with emphysema. *Pathophysiology* **8**, 215–221.

Mattson J.P., Delp M.D. & Poole D.C. (2004) Differential effects of emphysema on skeletal muscle fibre atrophy in hamsters. *Eur. Respir. J.* **23**, 703–707.

Miller G.L. (1959) Protein determination for larger numbers of samples. *Anal. Chem.* **31**, 964–968.

Oliveira F.J.A. & Cecchini R. (2000) Oxidative stress of liver in hamsters infected with Leishmania (L.) chagasi. *J. Parasitol.* **86**, 1067–1072.

Petty T.L. (2006) The history of COPD. *Int. J. Chron. Obstruct. Pulmon. Dis.* **1**, 3–14.

Powers S.K., Duarte J., Kavasis A.N. & Talbert E.E. (2010) Reactive oxygen species are signaling molecules for skeletal muscle adaptation. *Exp. Physiol.* **95**, 1–9.

Reznick A.Z. & Packer L. (1994) Oxidative damage to proteins: spectrophotometric method for carbonyl assay. *Methods Enzymol.* **233**, 357–363.

Rinaldi M., Maes K., De Vleeschauwer S. *et al.* (2012) Long-term nose-only cigarette smoke exposure induces emphysema and mild skeletal muscle dysfunction in mice. *Dis. Model Mech.* **5**, 333–341.

Schols A.M., Soeters P.B., Dingemans A.M., Motert R., Frantzen P.J. & Wouters E.F. (1993) Prevalence and characteristics of nutritional depletion in patients with stable COPD eligible for pulmonary rehabilitation. *Am Rev Respir Dis.* **147**, 1151–1156.

Schulz H., Mohr M. & Meyer M. (1989) Elastase and papain inhibition by serum of mammals. *Scand. J. Clin. Lab. Invest.* **49**, 381–388.

Swallow E.B., Reyes D., Hopkinson N.S. *et al.* (2007) Quadriceps strength predicts mortality inpatients with moderate to severe Chronic Obstructive Pulmonary Disease. *Thorax* **62**, 115–120.

Tietze F. (1969) Enzymic method for quantitative determination of nanogram amounts of total and oxidized glutathione: applications to mammalian blood and other tissues. *Anal. Biochem.* **27**, 502–522.

Tonon J., Cecchini A.L., Brunnquell C.R., Bernardes S.S., Cecchini R. & Guarnier F.A. (2013) Lung injury-dependent oxidative status and chymotrypsin-like activity of skeletal muscles in hamsters with experimental emphysema. *BMC Musculoskelet Disord.* **14**, 39.

Wijnhoven H.J., Heunks L.M., Geraedts M.C., Hafmans T., Viña J.R. & Dekhuijzen P.N. (2006) Oxidative and nitrosative stress in the diaphragm of patients with COPD. *Int J Chron. Obstruct. Pulm. Dis.* **1**, 173–179.

Wright J.L. & Churg A. (2002) A Model of Tobacco Smoke-Induced Airflow Obstruction in the Guinea Pig. *Chest* **121**, 188–191.

Wüst R.C.I. & Degens H. (2007) Factors contributing to muscle wasting and dysfunction in COPD patients. *Int. J. Chron. Obstruct. Pulmon. Dis.* **2**, 289–300.

Zhang X., Pang B., Hou X., Wang J. & Wang C. (2010) Oxidative stress and peripheral skeletal muscle dysfunction in rats with emphysema. *Chin Med J.* **123**, 40–44.